PTT Variability for Discrimination of Sleep Apnea Related Decreases in the Amplitude Fluctuations of PPG Signal in Children

Eduardo Gil*, Raquel Bailón, José María Vergara, and Pablo Laguna, *Senior Member, IEEE*

Abstract—In this paper, an analysis of pulse transit time variability (PTTV) during decreases in the amplitude fluctuations of pulse photoplethysmography signal (PPG) (DAP) events for obstructive sleep apnea syndrome (OSAS) screening is presented. The temporal evolution of time–frequency PTTV parameters during DAP was analyzed. The results show an increase in the sympathetic activity index low-frequency component (LF) during DAP for PTTV (85%) significantly higher than for heart rate variability (HRV) (33%), ($p < 10^{-13}$). However, decreases in parasympathetic activity produce lower decrements in high-frequency component (HF) indexes for PTTV (18%) than for HRV (22%). Thus, PTTV reflects sympathetic changes more clearly than HRV. A clinical study was carried out. DAP events were classified as apneic or nonapneic using a linear discriminant analysis from the PTTV indexes. The ratio of DAP events per hour r_{DAP}, the ratio after filtering based on HRV indexes $r_{\text{DAP}}^{\text{HRV}}$, or on PTTV indexes $r_{\text{DAP}}^{\text{PTTV}}$, were computed. The results show an accuracy of 75% for $r_{\text{DAP}}^{\text{PTTV}}$ (14% increase with respect to r_{DAP} and 5% increase with respect to $r_{\text{DAP}}^{\text{HRV}}$), a sensitivity of 81.8%, and a specificity of 73.9% when classifying 1-h polysomnographic excerpts as OSAS or normal. These results suggest that the combination of DAP and PTTV could be better alternative for sleep apnea screening using PPG with the added benefit of its low cost and simplicity.

Index Terms—Children, decreases in the amplitude fluctuations of pulse photoplethysmography signal (PPG) (DAP), PPG, pulse transit time variability (PTTV), sleep apnea, time–frequency.

I. INTRODUCTION

THE SPECTRUM of severity for sleep-disordered breathing ranges from minimal primary snoring to the more severe obstructive sleep apnea syndrome (OSAS). OSAS is characterized by recurrent airflow obstruction caused by total or partial collapse of the upper airway. These obstructive events lead to

*E. Gil is with the Communications Technology Group, Aragón Institute of Engineering Research, and CIBER de Bioingeniería, Biomateriales y Nanomedicina (CIBER_BBN), University of Zaragoza 50018 Zaragoza, Spain (e-mail: edugilh@unizar.es).

R. Bailón and P. Laguna are with the Communications Technology Group, Aragón Institute of Engineering Research, and CIBER de Bioingeniería, Biomateriales y Nanomedicina (CIBER_BBN), University of Zaragoza 50018 Zaragoza, Spain (e-mail: rbailon@unizar.es; laguna@unizar.es).

J. M. Vergara is with the Sleep Department, Miguel Servet Children Hospital, and CIBER de Bioingeniería, Biomateriales y Nanomedicina (CIBER_BBN), University of Zaragoza 50018 Zaragoza, Spain (e-mail: vergeur@comz.org).

oxygen desaturation, and an increase in mechanical respiratory efforts in order to reopen the upper airways. If these efforts are not sufficient and the hypercapnia level is dangerous, an arousal is generated to reactivate all the peripheral systems and respiration is restored.

These episodes may recur hundreds of times in a single night, with serious health implications [1]. The resulting sleep fragmentation [2] and blood gas modifications cause malfunctions of sleep-related restorative processes, and induce chemical and structural injuries in the cells of the central nervous system. Not only does this cause daytime sleepiness, it can in turn lead to systemic hypertension [3] and an increase in the likelihood of cardiovascular diseases [4]. Childhood is a critical time for acquiring core academic and social skills, and repeated failures related to sleep fragmentation at critical stages of development can fundamentally influence a child's motivation and behavior [5]–[7].

Diagnosis of OSAS is usually performed by polysomnography (PSG) in a sleep laboratory, consisting of the measurement and recording of several signals used to analyze sleep and breathing, whereas PSG represents the "gold standard" for the diagnosis, it is an expensive and time-consuming procedure. Given the high prevalence of OSAS [8] (4% for men, 2% for women, and 3% for children), its potential importance as a contributing factor to cardiovascular morbidity, and the availability of an effective treatment for this disease, several strategies have been developed to decrease the number of the sleep recordings, including sleep questionnaires, ambulatory recordings, simplified multichannel systems, and nocturnal oximetry [9].

One alternative to PSG is the pulse photoplethysmography signal (PPG). PPG, which was developed by Hertzman [10], is a simple and useful method for measuring the pulsatile component of the heartbeat and evaluating peripheral circulation, and is tie-related to arterial vasoconstriction or vasodilatation generated by the autonomic nervous system (ANS) and modulated by the heart cycle. When an apnea occurs, sympathetic activity increases as a response to the obstructive event in order to reestablish respiration. The increase in sympathetic activity is associated with vasoconstriction and is possibly related to transient arousal [11]–[15]. Vasoconstriction is reflected in PPG by a decrease in the signal amplitude fluctuation [16]–[18]. Several studies have analyzed the relationship between apnea and peripheral vasoconstriction for OSAS diagnosis [18]–[20].

Automatic detection of decreases in the amplitude fluctuations of PPG (DAP) have shown their utility for OSAS diagnosis [21]. Nevertheless, not all DAP events are associated with an

apnea. These events may be related to arousals not associated with apnea or other physiological events. Therefore, in a previous study [22], information about ANS, measured using HRV, was included in the diagnostic method, improving significantly the sensitivity and specificity of OSAS diagnosis by DAPs after discarding based on HRV parameters.

Spectral analysis of the HRV signal has been widely used for evaluating the action of the ANS. Power spectral density of the HRV exhibits oscillations, which are related to the parasympathetic and sympathetic activities [23]. The bandwidth of spectral components of the HRV goes from 0.003 to 0.5 Hz, where the range between 0.003 and 0.04 Hz (very low-frequency component, VLF) takes account of long-term regulation mechanisms. The range between 0.04 and 0.15 Hz (low-frequency component, LF) represents both sympathetic and parasympathetic modulation, although an increase in its power is generally associated with a sympathetic activation. However, even nowadays there is some controversy about the contribution of each autonomic branch to this frequency band. The 0.15–0.5 Hz range (high-frequency component, HF) corresponds to parasympathetic modulation and is synchronous with the respiratory rate. Finally, the LF to HF ratio is a concise index to evaluate the sympathovagal balance controlling HR.

On the other hand, PPG has been directly related to the cardiac function, giving as a result a measure of the pulse transit time (PTT) [24], [25]. PTT gives a quantitative measure of the time that the pulse wave needs for passing from one arterial, typically the aorta, to another, typically in the periphery, and is evaluated as the time interval between the ECG R peak and the corresponding PPG wave. Respiratory effort increases caused by apnea produces an increase in the amplitude oscillations of PTT [26]–[28]. PTT decreases after an apneic event due to a sympathetic activation related to arousal, which produces HR increment, higher stroke volume, and vasoconstriction, which in turn generate pulse wave acceleration [29]–[31]. Therefore, several studies have focused on detecting apnea by using the PTT signal, whether in adults [24], [32], [33] or children [34], [35].

It is well known that by far the most important part of the ANS for regulating the circulation is the sympathetic nervous system [36], [37]. Although the parasympathetic nervous system is exceedingly important for many other autonomic functions of the body, it plays only a minor role in the regulation of the circulation. Its most important circulatory effect is to control the HR by way of parasympathetic nerve fibers to the sinoatrial node in the vagus nerves. Blood vessels are, thus mainly innervated by sympathetic nerve fibers.

The aim of this study is to analyze the PTT variability (PTTV) during DAPs to evaluate its usefulness for rejecting DAP not related to apnea, and so increase specificity in the apnea detector. The hypothesis is that, as PTT, which reflects the peripheral circulation, is mainly mediated by sympathetic activity, the use of PTTV instead of HRV could increase the accuracy of DAP events for OSAS diagnosis after DAP rejection according to PTTV. To test this hypothesis, a comparison between apnea screening using only PPG, the combination of PPG and HRV, and the combination of PPG and PTTV is carried out. The analysis of PTTV during DAP events presented in this paper is
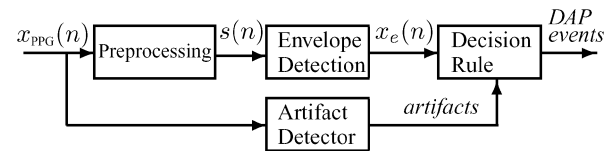

Fig. 1. DAP detector diagram.

analogous to the analysis of HRV during DAP events shown in [22]. Section II introduces materials and methods focused on PTTV analysis. Section III presents the results, which are discussed in Section IV. Finally, Section V presents the conclusions.

II. MATERIALS AND METHODS

A. Data

PSG recordings of 21 children over one complete night, the same dataset as employed in [22], were used in this study. The age range of the children is 4.47 ± 2.04 (mean$\pm$S.D.) years. The children were referred to the Miguel Servet Children's Hospital in Zaragoza for suspected sleep-disordered breathing. EEG electrode positions C3, C4, O1, and O2, chin electromyogram, ECG leads I and II, eye movements, airflow, and chest and abdominal respiratory efforts were recorded by a digital polygraph (BITMED EGP800), according to the standard procedure defined by the American Thoracic Society [38]. PPG and arterial oxygen saturation (SaO$_2$) were measured continuously using a pulse oximeter (COSMO ETCO2/SpO2 Monitor Novametrix, Medical Systems). Signals were stored with a sample rate of 100 Hz, except ECG signals, which were sampled at 500 Hz. OSAS evaluation from PSG data were scored by clinical experts using the standard procedures and criteria [8]. Ten children were diagnosed with OSAS and 11 were diagnosed as normal.

B. DAP Clustering Criteria Related to Apnea Signs

PPG signal was analyzed using the method described in [21] for DAP detection. This detector is based on a preprocessor stage, which suppress the mean, an envelope detection using root mean square technique, and a decision rule based on an adaptive threshold. The detector also includes an artifact detector stage based on Hjorth parameters, see Fig. 1.

Segments from ECG, PPG, SaO$_2$, air flow, and abdominal effort centered at the DAP event onset and lasting 5 min were extracted, and from here denoted as DAP events. DAP events, when analyzed together with respiratory and SaO$_2$ signals, do not always present well-defined patterns in the sense of being or not being associated with oxygen desaturation or apnea. To avoid these uncertainties in defining a training set, a subset of DAP events with well-defined signatures, related to apnea or oxygen desaturation, were selected and sorted into five different groups with uniform patterns based on the gold standard criterion for defining sleep apneas [8]. The DAP events were classified into group 1 (G$_1$) when SaO$_2$ decreases by at least 3% and there is no clear reduction in the airflow signal, group 2 (G$_2$) when the airflow decreases by at least 50% with respect to the baseline
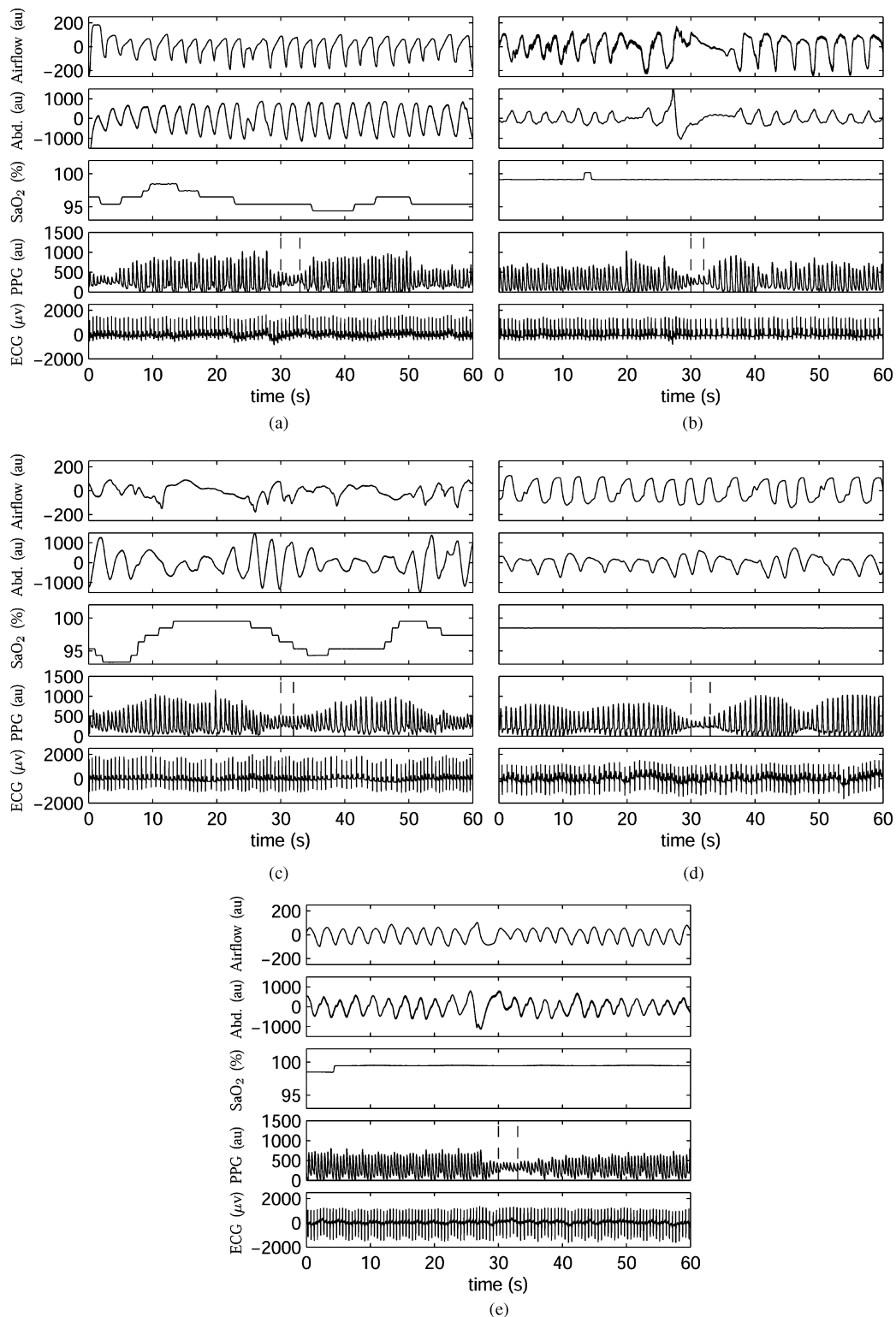
Fig. 2. DAP events examples. The DAP event onset and end (as given by the detector) are marked with dashed lines. (a) G_1. (b) G_2. (c) G_3. (d) G_4. (e) G_5.

for a minimum duration of 5 s and there is no reduction in SaO_2, group 3 (G_3) when the airflow reduces by more than 50% from the baseline and is accompanied by a reduction in SaO_2 of at least 3%, group 4 (G_4) when the DAP event correlates neither to the airflow reduction nor the SaO_2 decrement, and finally, group 5 (G_5) when the DAP event is related neither

to apneas nor to SaO_2 decrements, but a change in respiration occurs. Fig. 2 shows typical examples of airflow, abdominal effort, SaO_2, PPG, and ECG for the different groups. G_1, G_2, and G_3 can be merged into a single group named G_a (apneic group), while G_4 and G_5 can also be regrouped into a single set G_n (nonapneic group). A total of 268 DAP events were

TABLE I
NUMBER OF DAP EVENTS IN EACH GROUP

Clinical	DAP group					
Diagnosis	G_1	G_2	G_3	G_4	G_5	Total
Normal	4	32	5	76	31	148
OSAS	44	21	33	11	11	120
Total	48	53	38	87	42	268

extracted. Table I shows a summary of the DAP events in each group.

C. Variability Analysis

HRV and PTTV were obtained in order to evaluate the ANS. An automatic QRS detector [39] was applied to the ECG signal providing the θ_j beat location for every jth beat.

1) HR: The inverse interval function $d_{\mathrm{IIF}}(\theta_j)$ denoting the HR time series was extracted from the ECG segments

$$d_{\mathrm{IIF}}(\theta_j) = \frac{1}{\theta_j - \theta_{j-1}} \qquad (1)$$

and the evenly sampled signal $d_{\mathrm{IIF}}(m)$ at 2 Hz was subsequently, generated using a cubic spline interpolation.

2) PTT: The following process was applied for obtaining the PTT signal. For every jth beat a PTT value was calculated. First of all, the PPG signal was interpolated using cubic splines to increase the resolution in time up to an equivalent sampling rate of 500 Hz, obtaining the $x_{\mathrm{PPG}}(k)$ signal. Therefore, PTTV and HRV have the same time resolution. Then, the occurrence time of the pulse wave peak k_{p_j} was detected starting from 150 ms after QRS complex (sample $\theta_j + 75$)

$$k_{p_j} = \arg \max_k [x_{\mathrm{PPG}}(\theta_j + 75), \ldots, x_{\mathrm{PPG}}(k), \ldots, x_{\mathrm{PPG}}(\theta_{j+1})]. \quad (2)$$

The PPG pulse wave onset k_{o_j} was then detected

$$k_{m_j} = \arg \min_k [x_{\mathrm{PPG}}(\theta_j), \ldots, x_{\mathrm{PPG}}(k), \ldots, x_{\mathrm{PPG}}(k_{p_j})] \quad (3)$$

$$k_{o_j} = \begin{cases} k_{m_j} & \text{if } \dfrac{\partial^2 x_{\mathrm{PPG}}(k)}{\partial k^2} < 0.03 \\ \text{else } \arg \min_k \left[\dfrac{\partial^2 x_{\mathrm{PPG}}(k)}{\partial k^2} \right] > 0.03 \end{cases} \forall k \in \{k_{m_j}, \ldots, k_{p_j}\}.$$

$$(4)$$

The 0.03 threshold was empirically determined. Finally, the PPG wave reference point k_{r_j} was calculated

$$k_{r_j} = \arg \min_k \left[x_{\mathrm{PPG}}(k) \ge x_{\mathrm{PPG}}(k_{o_j}) + \frac{x_{\mathrm{PPG}}(k_{p_j}) - x_{\mathrm{PPG}}(k_{o_j})}{2} \right]. \quad (5)$$

Thus, the PTT value for each jth beat, $d_{\mathrm{PTT}}(\theta_j)$ is as follows:

$$d_{\mathrm{PTT}}(\theta_j) = k_{r_j} - \theta_j. \qquad (6)$$

PTT values for each beat $d_{\mathrm{PTT}}(\theta_j)$, out of the range [150 and 400 ms] were considered invalid. Finally, the PTT time series was resampled at 2 Hz by cubic spline interpolation in order to obtain an evenly sampled signal $d_{\mathrm{PTT}}(m)$. Fig. 3 shows an example of the process applied to obtain the PTT signal. Once the R peak wave is detected in the ECG signal, the PPG pulse
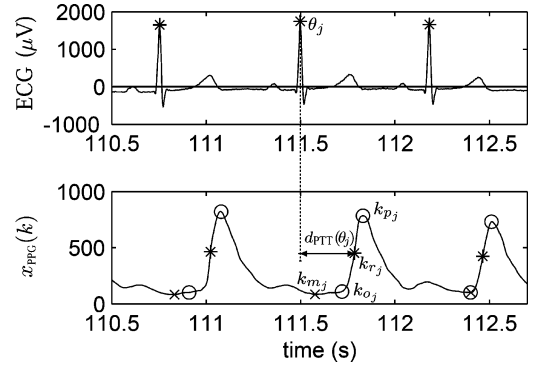

Fig. 3. PTT measure example.

wave peak k_{p_j} is detected within 150 ms after the j beat and previous to the next beat. Afterward the minimum value of $x_{\mathrm{PPG}}(k)$ within θ_j and k_{p_j} is obtained as a possible PPG wave onset reference k_{o_j}. The k_{o_j} reference is corrected based on abrupt changes in the PPG signal, determined with a threshold in the second derivative (see first and second beat in Fig. 3). The k_{o_j} is not corrected in the third beat. Finally, the pulse arrival at the periphery is measured as 50% peak value of the PPG wave.

3) Time–frequency transformation: Time–frequency representation was used to decompose both signals $d_{\mathrm{IIF}}(m)$ and $d_{\mathrm{PTT}}(m)$ in their different frequencies at each time. Details of time–frequency transformation, where smooth pseudo Wigner–Ville distribution was used, are shown in [22] and [40]. The time evolution of PTTV and HRV indexes were then evaluated, total power from 0.0033 to 0.5 Hz ($\mathcal{P}_{\mathrm{T}}^{\mathrm{X}}(m)$), VLF power from 0.0033 to 0.04 Hz ($\mathcal{P}_{\mathrm{VLF}}^{\mathrm{X}}(m)$), LF power from 0.04 to 0.15 Hz ($\mathcal{P}_{\mathrm{LF}}^{\mathrm{X}}(m)$), HF power from 0.15 to 0.5 Hz ($\mathcal{P}_{\mathrm{HF}}^{\mathrm{X}}(m)$), LF to HF ratio ($\mathcal{R}_{\mathrm{LF/HF}}^{\mathrm{X}}(m)$), and their normalized versions with respect to the total power $\mathcal{P}_{\mathrm{VLF}_n}^{\mathrm{X}}(m)$, $\mathcal{P}_{\mathrm{LF}_n}^{\mathrm{X}}(m)$, and $\mathcal{P}_{\mathrm{HF}_n}^{\mathrm{X}}(m)$, superscript $X \in \{\mathrm{HRV, PTTV}\}$.

D. Statistical Analysis and Classification

1) Statistical Analysis: In order to quantify the evolution of autonomic variations when a DAP event is associated or not associated to airflow decrements, $\mathrm{SaO_2}$ reductions or to nothing, four time windows were defined in specific time intervals related to the onset of DAP events. Fig. 4 shows the mean of the $d_{\mathrm{PTT}}(m)$ sequences and the mean of their corresponding time–frequency maps when the DAP is related or not related to an apneic episode, as well as the windows defined in relation to a DAP event. Time 0 s is assigned to the DAP onset. The time windows are defined as follows: 1) reference window (w_r) is located 15 s previous to the DAP event onset with a duration of 5 s; 2) DAP episode window (w_d) is found 2 s before the DAP onset and lasting 5 s; 3) postDAP event window (w_p) located 15 s after DAP onset and lasting 5 s; and 4) global window (w_g) starting at 20 s previous to the DAP onset, lasting 40 s, and containing the others windows.

In order to reduce the biovariability in $d_{\mathrm{PTT}}(m)$ temporal indexes, the signal was first normalized by subtracting the mean value and dividing by the variance during the 2 min
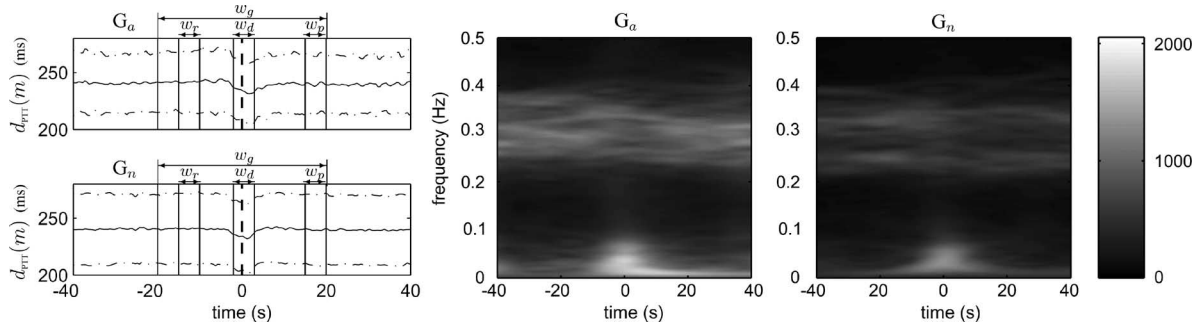
Fig. 4. $d_{\mathrm{PTT}}(m)$ mean $\pm$ S.D. and mean time–frequency maps for apneic ($\mathrm{G}_a \equiv \mathrm{G}_1 + \mathrm{G}_2 + \mathrm{G}_3$) and nonapneic ($\mathrm{G}_n \equiv \mathrm{G}_4 + \mathrm{G}_5$) DAP events. Analysis windows. Dashed line at reference time indicate DAP onset.

around the DAP event $d_{\mathrm{PTT}_n}(m)$. Mean absolute values in the time windows were computed for $d_{\mathrm{PTT}_n}(m)$, $\mathcal{P}_{\mathrm{LF}_n}^{\mathrm{PTTV}}(m)$, $\mathcal{P}_{\mathrm{HF}_n}^{\mathrm{PTTV}}(m)$, and $\mathcal{R}_{\mathrm{LF/HF}}^{\mathrm{PTTV}}(m)$, and the variance of $d_{\mathrm{PTT}_n}(m)$, obtaining the indexes $\overline{\mathrm{PTT}}_n^w$, $\overline{\mathcal{P}}_{\mathrm{LF}_n}^{\mathrm{PTTV}^w}$, $\overline{\mathcal{P}}_{\mathrm{HF}_n}^{\mathrm{PTTV}^w}$, $\overline{\mathcal{R}}_{\mathrm{LF/HF}}^{\mathrm{PTTV}^w}$, and $\sigma_{\mathrm{PTT}_n}^w$, respectively, for each window $w \in \{w_r, w_d, w_p, w_g\}$. The Kruskal–Wallis nonparametric statistic approach was performed in two cases: one, to compare the time variations among windows of PTTV parameters, and the other to compare differences among groups for each parameter and window. *Post hoc* analysis was applied to determine, which pairs had statistical differences ($p < 0.05$).

2) Features Sets: The set of indexes formed by the mean and the variance within the four different windows ($\overline{\mathrm{PTT}}^w$, σ_{PTT}^w, $\overline{\mathcal{P}}_{\mathrm{VLF}_n}^{\mathrm{PTTV}^w}$, $\overline{\mathcal{P}}_{\mathrm{LF}_n}^{\mathrm{PTTV}^w}$, $\overline{\mathcal{P}}_{\mathrm{HF}_n}^{\mathrm{PTTV}^w}$, and $\overline{\mathcal{R}}_{\mathrm{LF/HF}}^{\mathrm{PTTV}^w}$) were extracted from the groups (G_a and G_n) in order to select a set that could provide separation between normal (apneic unrelated) and apneic (apneic related) DAP events. In addition, the difference between reference w_r and DAP episode window w_d, as well as between w_r and postDAP event window w_p, was computed and denoted as $\Delta Y^{w_1 - w_2}$, where Y is the main index, with $Y \in \{\overline{\mathrm{PTT}}, \sigma_{\mathrm{PTT}}, \overline{\mathcal{P}}_{\mathrm{VLF}_n}^{\mathrm{PTTV}}, \overline{\mathcal{P}}_{\mathrm{LF}_n}^{\mathrm{PTTV}}, \overline{\mathcal{P}}_{\mathrm{HF}_n}^{\mathrm{PTTV}}, \overline{\mathcal{R}}_{\mathrm{LF/HF}}^{\mathrm{PTTV}}\}$, and the superscripts w_1 and w_2 denote the two windows involved (w_r for reference, w_d for DAP episode, and w_p for postDAP event). A total of 34 features were extracted.

3) Classifier and Selection of Features: A linear discriminant analysis was used to distinguish between DAP events related and unrelated to apnea episodes (G_a and G_n). For training the classifier, DAP events in Section II-B selected from groups G_1 to G_5 were used. The wrap method was used for feature selection. Details are shown in [22].

E. Clinical Study

To evaluate the improvement for OSAS diagnosis based on PPG achieved by adding PTTV information, a clinical study was carried out analogous to that presented in [22]. The available one night PSG recordings described in Section II-A were split into 1-h length fragments. These 1-h PSG fragments were labeled as control, doubt, or pathologic according to SaO_2 desaturation in order later to be able to evaluate the classifier accuracy for these fragments. To establish these distinctions, a baseline level β corresponding to the SaO_2 signal mode of the entire night

TABLE II
PSG FRAGMENTS CLASSIFICATION

Clinical diagnosis	# subjects	# fragments	PSG fragments classification		
			# normal	# doubt	# pathologic
Normal	10	42	41	1	0
Pathologic	11	52	23	19	10
Total	21	94	64	20	10

recording was considered. In all the recordings $\beta \geq 97\%$. Total time intervals with the SaO_2 signal below $\beta - 3\%$, $t_{\beta-3}$, was calculated for each fragment. The PSG fragments were classified according to the following criteria:

$$t_{\beta-3} < 0.9 \text{ min}, \quad \text{control}$$
$$0.9 \text{ min} < t_{\beta-3} < 3 \text{ min} \quad \text{doubt}$$
$$t_{\beta-3} > 3 \text{ min} \quad \text{pathologic}. \quad (7)$$

This implies a minimum of 5% of the time with evident oxygen desaturation to be considered as pathologic, which corresponds to a severe OSAS criteria in children [41] of 18 apneas/h having a mean duration of 10 s. For the control group, the threshold corresponds to 5 apneas/h. Table II shows the classification of these PSG fragments.

Now the objective is to classify these 1-h fragments according to the following three indexes.

1) The number of DAP events per hour ratio, as described in [21], r_{DAP}.
2) The number of apneic DAP events per hour ratio, considered as apneic based on HRV according to the methodology presented in [22], $r_{\mathrm{DAP}}^{\mathrm{HRV}}$.
3) The number of apneic DAP events per hour ratio, considered as apneic based on PTTV classification according to the methodology presented in Section II-D, $r_{\mathrm{DAP}}^{\mathrm{PTTV}}$.

Leave-one-out method was used for testing the classifier. In each iteration of the algorithm one PSG fragment is excluded of the training set and receiver operating characteristic (ROC) curves were calculated for the three indexes (r_{DAP}, $r_{\mathrm{DAP}}^{\mathrm{HRV}}$, and $r_{\mathrm{DAP}}^{\mathrm{PTTV}}$). Next the optimum thresholds in this iteration were determined in terms of minimizing the euclidean distance between them and the optimal point sensitivity (Se) = 1 and specificity (Sp) = 1. Then, the PSG fragment excluded was classified based on these thresholds and considered as true positive (TP), false positive (FP), true
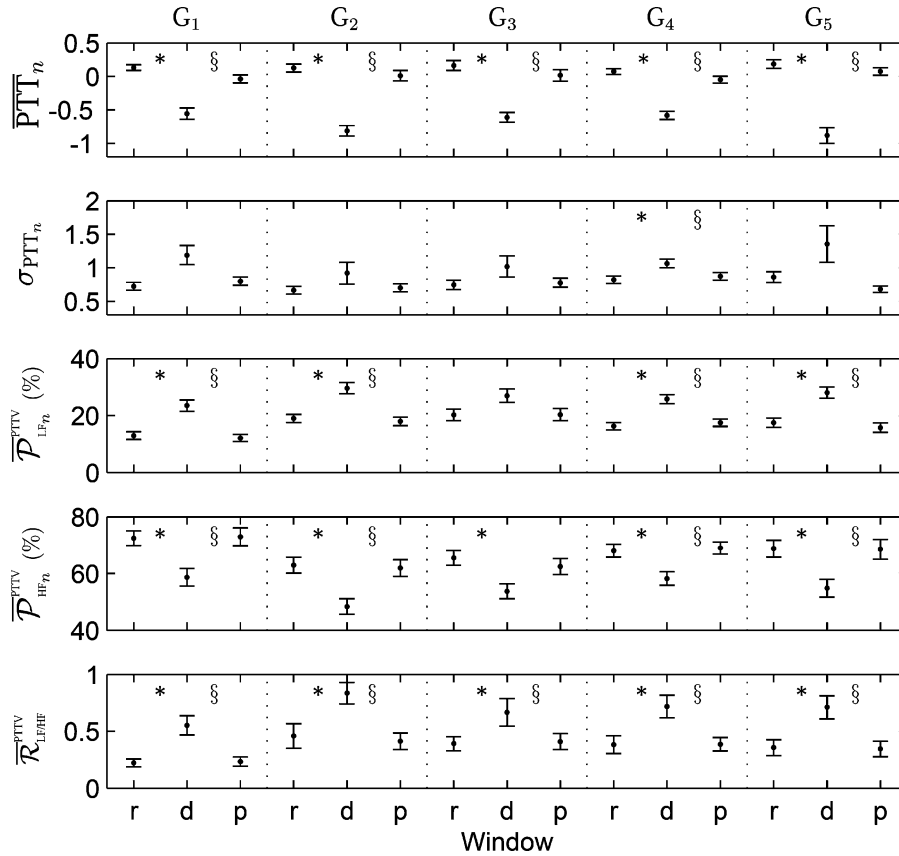
Fig. 5.　$\overline{\mathrm{PTT}}_n \pm \mathrm{SE}$, $\sigma_{\mathrm{PTT}_n} \pm$, SE and spectral indexes obtained by smooth pseudo Wigner–Ville distribution. The letters refer to the temporal windows analyzed during DAP. From the top to the bottom, mean PTT ($\overline{\mathrm{PTT}}_n$), standard deviation PTT (σ_{PTT_n}), LF ($\overline{\mathcal{P}}_{\mathrm{LF}_n}^{\mathrm{PTTV}}$), HF ($\overline{\mathcal{P}}_{\mathrm{HF}_n}^{\mathrm{PTTV}}$), and LF to HF ratio ($\overline{\mathcal{R}}_{\mathrm{LF/HF}}^{\mathrm{PTTV}}$) of PTT. All the spectral parameters were normalized with respect to the total power at each time. * refers to $p < 0.05$ between windows w_r and w_d, and § to $p < 0.05$ between windows w_d and w_p.

negative (TN), or false negative (FN) depending on the reference. These steps are repeated for all 1-h PSG fragments and the performance of the classifier is calculated. In addition, Wilcoxon nonparametric statistical analysis was carried out for all the indexes in order to evaluate their discriminant power between groups.

When we are interested in having a label attached to a patient, we need a rule to determine when a patient with a given number of pathological fragments is considered as a pathologic subject. To do this, the percentage of time under pathologic fragments based on r_{DAP}, $r_{\mathrm{DAP}}^{\mathrm{HRV}}$, and $r_{\mathrm{DAP}}^{\mathrm{PTTV}}$ was analyzed. The threshold for this percentage was selected for maximizing Se and Sp. From the total of 21 children, six subjects were excluded because only less than 4 h had ECG and PPG signals of acceptable quality; therefore, 15 registers were included in this study corresponding to eight OSAS and seven normal according to clinical diagnosis.

III. RESULTS

A. Statistical Analysis Results

Fig. 5 shows mean and standard error of $\overline{\mathrm{PTT}}_n$, σ_{PTT_n}, and spectral indexes obtained by smooth pseudo Wigner–Ville dis-

tribution. The letters refer to the temporal windows analyzed during DAP (r: reference, d: DAP episode, and p: postDAP event). * refers to $p < 0.05$ between windows w_r and w_d, and § to $p < 0.05$ between windows w_d and w_p. Table III shows the mean percentage variation of frequency index during DAP events for HRV and PTTV analysis.

The best features to classify between G_a and G_n obtained by the wrap method were $\sigma_{\mathrm{PTT}}^{w_g}$, $\overline{\mathcal{P}}_{\mathrm{VLF}_n}^{\mathrm{PTTV}^{w_d}}$, and $\Delta\overline{\mathcal{P}}_{\mathrm{VLF}_n}^{\mathrm{PTTV}^{w_r - w_d}}$, having an accuracy Acc = 66%, a $Se = 58\%$, and a $Sp = 75\%$.

B. Clinical Study Results

The results regarding PSG fragments and subject classification are shown in Table IV. The inclusion of PTTV information improves the PSG fragment classification accuracy in 5% with respect to $r_{\mathrm{DAP}}^{\mathrm{HRV}}$ and 14% with respect to r_{DAP}.

Values of Acc = 75%, $Se = 81.8\%$, and $Sp = 73.9\%$ are obtained by the $r_{\mathrm{DAP}}^{\mathrm{PTTV}}$ index. The ROC curves for the training set in Fig. 6, varying thresholds in r_{DAP}, $r_{\mathrm{DAP}}^{\mathrm{HRV}}$, and $r_{\mathrm{DAP}}^{\mathrm{PTTV}}$, demonstrate the advantage of including the PTTV information. The optimum threshold values for r_{DAP}, $r_{\mathrm{DAP}}^{\mathrm{HRV}}$, and $r_{\mathrm{DAP}}^{\mathrm{PTTV}}$ are 5.13, 3.05, and 3.04, respectively. The AUC for PTTV increase by about 10% with respect to HRV and DAP only

TABLE III
MEAN ± S.D. PERCENTAGE VARIATION OF FREQUENCY INDEX DURING DAP

%	$\dfrac{\Delta\overline{\mathcal{P}}_{LF_n}^{HRV^{wd}-wr}}{\overline{\mathcal{P}}_{LF_n}^{HRV^{wr}}}$	$\dfrac{\Delta\overline{\mathcal{P}}_{LF_n}^{PTTV^{wd}-wr}}{\overline{\mathcal{P}}_{LF_n}^{PTTV^{wr}}}$	p	$\dfrac{\Delta\overline{\mathcal{P}}_{HF_n}^{HRV^{wd}-wr}}{\overline{\mathcal{P}}_{HF_n}^{HRV^{wr}}}$	$\dfrac{\Delta\overline{\mathcal{P}}_{HF_n}^{PTTV^{wd}-wr}}{\overline{\mathcal{P}}_{HF_n}^{PTTV^{wr}}}$	p	$\dfrac{\Delta\overline{\mathcal{R}}_{LF/HF}^{HRV^{wd}-wr}}{\overline{\mathcal{R}}_{LF/HF}^{HRV^{wr}}}$	$\dfrac{\Delta\overline{\mathcal{R}}_{LF/HF}^{PTTV^{wd}-wr}}{\overline{\mathcal{R}}_{LF/HF}^{PTTV^{wr}}}$	p
G_1	41.7±59.4	118.8±120.7	$8\cdot10^{-5}$	-22.7±47.8	-20.1±18.9	0.061	146.3±184.0	203.1±206.6	0.095
G_2	44.4±66.9	75.7±88.0	0.035	-37.2±34.6	-19.9±34.2	0.001	222.3±295.2	156.5±165.8	0.458
G_3	18.3±44.0	55.2±74.3	0.016	-8.8±67.2	-17.0±21.6	0.630	81.3±155.0	105.9±117.7	0.134
G_4	30.0±52.4	80.0±88.2	$5\cdot10^{-6}$	-13.9±26.8	-14.9±21.0	0.954	71.8±98.8	134.9±147.2	0.002
G_5	25.3±43.6	97.6±88.6	$5\cdot10^{-5}$	-29.0±34.6	-17.9±32.3	0.054	123.4±131.1	171.5±137.0	0.091
G_a	36.4±59.4	84.4±99.7	$1\cdot10^{-6}$	-24.5±50.7	-19.2±26.3	$8\cdot10^{-4}$	157.5±232.5	157.9±172.6	0.229
G_n	28.4±49.6	85.6±88.4	$1\cdot10^{-9}$	-18.9±30.3	-15.8±25.0	0.277	88.6±112.5	146.6±144.5	$6\cdot10^{-4}$
G_T	**32.6±55.0**	**85.0±94.1**	**$2\cdot10^{-14}$**	**-21.8±42.2**	**-17.5±25.7**	**0.002**	124.3±187.6	152.3±159.1	0.001

TABLE IV
PSG FRAGMENTS CLASSIFICATION RESULTS

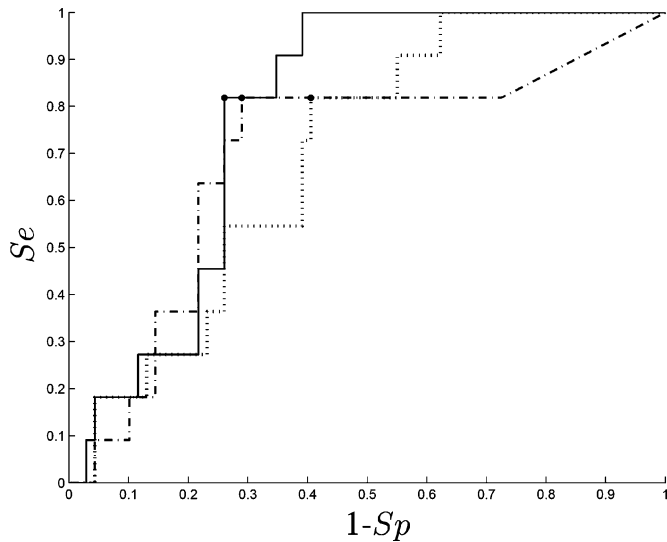| Index	PSG Fragments classification				Subjects classification		
	Se (%)	Sp (%)	Acc (%)	AUC (%)	Se (%)	Sp (%)	Acc (%)
r_{DAP}	72.7	59.4	61.2	69.7	75	71.4	73.3
r_{DAP}^{HRV}	72.7	69.6	70.0	69.4	87.5	71.4	80
r_{DAP}^{PTTV}	81.8	73.9	75	78.1	75	85.7	80

Fig. 6. ROC curves for r_{DAP} (dotted line), r_{DAP}^{HRV} (dashed–dotted line), and r_{DAP}^{PTTV} (solid line). Bullet dots indicate the points, where the global results are presented.

analysis. In addition, the Wilcoxon statistic analysis shows a higher discriminant power between pathologic and normal for r_{DAP}^{PTTV} ($p = 0.0023$) than for r_{DAP}^{HRV} ($p = 0.0382$) and r_{DAP} ($p = 0.0372$). As for subject classification, the inclusion of HRV and PTTV variability improves the accuracy by 6.7%.

IV. DISCUSSION

An analysis of autonomic control derived from PTTV during DAP in children was presented and compared with HRV. Fig. 5 shows decrements in the $d_{PTT}(m)$ signal during DAP events associated with apnea (G_a), in agreement with [26], [30], [33]–[35]. However, these decrements also occur during DAP events without apneic association (G_n), which implies that the detection of decreases in PTT alone provides a poor specificity for apnea detection, as was reported by Poyares et al. [30]. The

time evolution of frequency features shows similar patterns in all groups, an increase in $\overline{\mathcal{P}}_{LF_n}^{PTTV}$ and $\overline{\mathcal{R}}_{LF/HF}^{PTTV}$, and a decrease in $\overline{\mathcal{P}}_{HF_n}^{PTTV}$ during DAP, indicating an activation of the sympathetic branch of the ANS followed by a recovery period. This time evolution of frequency parameters is similar to the HRV-based frequency analysis presented in [22], corroborating our previous results. Although PTTV studies hardly exist in frequency domain [42], a definition of frequency bands and their physiological meaning similar to the classical used in HRV presents coherent results because both indexes show the same pattern.

Table III shows the mean percentage variation of frequency indexes during DAP events. The increase in the sympathetic activity index for PTTV $\overline{\mathcal{P}}_{LF_n}^{PTTV}$, (85%) is significantly higher ($p < 10^{-13}$) than for HRV $\overline{\mathcal{P}}_{LF_n}^{HRV}$, (33%) during DAP, which means that PTTV reflects sympathetic changes between different physiological conditions (previous to DAP and during DAP) more clearly than HRV, confirming our hypothesis. This change could be argued to be due to high noise at some signal, however the low p-value makes us to state that some systematic behavior exists, which can be exploit. On the other hand, decreases in parasympathetic activity during DAP events produce lower decrements in parasympathetic activity indexes for PTTV $\overline{\mathcal{P}}_{HF_n}^{PTTV}$, (18%) than for HRV $\overline{\mathcal{P}}_{HF_n}^{HRV}$, (22%).

However, frequency indexes of PTTV are not useful in classifying DAP events as apneic or nonapneic because sympathetic activation is also present in nonapneic DAP events. All the indexes show similar values for all groups, see Fig. 5, and no significant differences were found in the Kruskal–Wallis statistical analysis when comparing differences among groups for each parameter and window, except for σ_{PTT} parameters ($p = 2 \times 10^{-10}$ for σ_{PTT}^{wg}), in agreement with [35]. This was, therefore, the first parameter selected by the wrap method in the selection of features process. Variability in the PTT signal is higher in the apneic group (G_a) than in the nonapneic group (G_n), which may be caused by an increase in respiratory effort as reported in [26]–[28].

The clinical study has shown that including information about ANS increases the accuracy of DAP events for PSG fragment classification, confirming our previous results [22]. Deriving this information from PTTV (r_{DAP}^{PTTV}) produces an increase in the accuracy of PSG fragment classification of 5% with respect to HRV (r_{DAP}^{HRV}). In addition, the index r_{DAP}^{PTTV} presents an increase of 9% in AUC for classifying 1-h polysomnographic events with respect to r_{DAP}^{HRV}, which means that detection based on r_{DAP}^{PTTV} is

more robust than that based on $r_{\mathrm{DAP}}^{\mathrm{HRV}}$, and less dependent on detector parameters. When two indexes have the same S_e and S_p, the one with higher AUC is less affected by threshold changes with respect to the optimum. So when the optimum threshold is not selected, the classifier performance in terms of S_e and S_p is less diminished. As for subjects classification results in terms of S_e, S_p, and Acc were the same for $r_{\mathrm{DAP}}^{\mathrm{HRV}}$ and $r_{\mathrm{DAP}}^{\mathrm{PTTV}}$. So this means that the potential advantages of PTTV are more linked to detail temporal analysis (1-h fragment) than for overall patient screening. In this study, HRV or PTTV have been considered separately. If HRV and PTTV have different autonomic information, as results in Table III seems to show, the combination of both features could give additional improvement, which is worth to try in a future study.

A limitation of our study is that oximetry has been used as the reference for 1-h PSG fragments. According to American Sleep Disorders Association criteria [9], oximetry is not sufficiently accurate or validated to recommend for use in OSAS diagnosis. Nevertheless, all pathologic fragments defined according to (7) correspond to children suffering from OSAS, see Table II and subjects classification use clinical diagnosis as the reference.

It is worth noting that the subset of DAP (G_a and G_n), where the discarding rules are trained, are included in the patients to be classified later on. Thus, even with different classifying objectives (one deciding on DAP origin and another on classifying patients), some bias could be introduced.

It is well established that PPG measurements are quite sensitive to patient and/or probe-tissue movement artifact. The automatic detection of such motion artifact and its separation from good quality although highly variable pulse recordings, is a nontrivial exercise in computer signal processing [43]. Movement artifacts detection in OSA diagnostic methods is very important because movements during arousal caused by apnea are frequent. So our DAP detector includes an artifact detector based on Hjorth parameters [21]. Other common source of error is muscular noise, which affects ECG signal and the accuracy of beat detection. To avoid this problem we used a QRS detector based on wavelet transform, which is robust to muscular noise [39]. Using a multiscale approach, it permits to attenuate noise at rough scales, and then to refine the precision.

Our main findings are as follows. An increase in sympathetic activity occurs during DAP events, in concordance with [17] and [22]. The increase in sympathetic activity is more evident in PTTV than in HRV so PTTV is a promising technique for ANS analysis, corroborating our main hypothesis. However, this difference in frequency analysis is not useful for improving PSG fragment classification because a sympathetic increase also exists in nonapneic DAP events. Nevertheless, temporal parameters of PTTV show significant differences for classification among groups. Thus, the inclusion of ANS information improves the PSG fragment classification, and PTTV indexes are more robust and less detector parameter-dependent than HRV indexes.

The photoplethysmography signal carries information related to the cardiovascular function as well as blood gas concentrations. This signal has interesting characteristics that can be used to detect apneic episodes. On the other hand, another electrophysiological signal extensively studied for apnea diagnosis is ECG. HRV analysis has become an important tool in assessing the human ANS. In addition, PTT is related with both PPG and ECG signals. PTT can generally refer to the time difference for a pulse wave to travel between two arterial sites. The speed at which this arterial pressure wave travels is directly proportional to blood pressure. A notable rise in blood pressure causes the vascular tone to increase, and hence, the arterial wall becomes stiffer, causing the PTT to shorten. For ease of measurement, the R-wave of the ECG has been used as the starting point, as it corresponds approximately to the opening of the aortic valve. Conventionally, the 25% or 50% point of the maximum value on the PPG pulse waveform is taken to indicate the arrival of the pulse wave. In this study, 50% was the reference used, see (5). Using the ECG R-wave as a starting point is convenient and easily identifiable, but this introduces an inaccuracy as there is a short delay between the occurrence of the R-wave and the opening of the aortic valve. This delay is also known as the isometric contraction time or preejection period (PEP) [33]. Although the PTT signal has been widely explored in recent years, very few studies have analyzed the PTTV within a time–frequency approach [42]. Our work has shown that PTTV analysis is a promising technique for evaluating the sympathetic branch of ANS, which can be applied in many clinical fields. Nevertheless, extended studies are needed to determine the precise link between PTTV and ANS.

Similar comments to those in [22] can be made, where our results fall within the reported interrater reliabilities for sleep scoring [44], where the mean epoch by epoch agreement between five scorers was 73%, and within the interobserver agreement on apnea-hypopnea index (AHI) using portable monitoring of respiratory parameters [45], where the AHI agreement scored by eight physicians was 73% measured by intraclass correlation coefficient.

Many studies have been carried out for OSAS screening attempting to reduce PSG cost and complexity. Different techniques have been proposed, oximetry-based screening being one of the most widely suggested for both the adult and pediatric population. Although these methods have high sensitivity, they tend to have very low specificity [9]. In addition, a confounding factor in children is that obstructive events frequently do not lead to significant oxyhemoglobin desaturation. Pulse oximetry in children has the same limitation as in adults [46]. Brouillette *et al.* [47], in an extensive study involving 349 children, obtained a positive predictive value of 97%, but the negative predictive value was only 53%. Other approaches based on ECG [48] have shown very good results for adults, achieving perfect scores of 100% in accuracy for subject classification. However, few ECG-based studies are aimed at children, for whom the physiology is different and important differences in sleep disorders exist [38], [41]. Shouldice *et al.* [49] reported a sensitivity of 85.7% and a specificity of 81.8% in an ECG-based study on children by adapting previous research on adults, where information about ECG-derived respiratory signals was included. Cardiorespiratory sleep studies that typically include two or more signals have also been considered. These studies have been shown to

be sensitive to OSAS, but mostly in adults [50]. There are other alternatives, such as nap studies, clinical history, sonography, or videography [46].

In summary, in terms of sensitivity and specificity, the results of our proposed method are similar to [49] or better than currently investigated alternatives for OSAS screening in children [46], [47], [51]. However, performance improvement to reach the levels of accuracy of adult methods would be desirable, and extended studies are needed to corroborate the potential of our method in diagnosing sleep disorders in children.

V. CONCLUSION

In conclusion, an analysis has been made of autonomic control derived from PTTV during DAP in children. Our results show a significant increase in LF and decrease in HF during DAP events for PTTV, indicating an increase in the sympatho-vagal balance of the ANS followed by a recovery period. Frequency indexes derived from PTTV reflect sympathetic changes more clearly than HRV. The $\overline{\mathcal{P}}_{\mathrm{LF}_n}^{\mathrm{HRV}}$ mean increase during all DAP events analyzed was 32.6%, whereas the $\overline{\mathcal{P}}_{\mathrm{LF}_n}^{\mathrm{PTTV}}$ mean increase was 85%. However, decreases in parasympathetic activity during DAP events produce lower decrements in parasympathetic activity indexes $\overline{\mathcal{P}}_{\mathrm{HF}_n}^{\mathrm{PTTV}}$ for PTTV (18%) than for $\overline{\mathcal{P}}_{\mathrm{HF}_n}^{\mathrm{HRV}}$ for HRV (22%).

A clinical study was carried out to evaluate the improvement in OSAS diagnosis based on PPG by adding PTTV information. DAP events were classified as apneic or nonapneic using a linear discriminant analysis from the PTTV indexes. The results show an accuracy of 75% for $r_{\mathrm{DAP}}^{\mathrm{PTTV}}$ (14% increase with respect to r_{DAP} and 5% increase with respect to $r_{\mathrm{DAP}}^{\mathrm{HRV}}$), a sensitivity of 81.8% and a specificity of 73.9% when classifying 1-h polysomnographic excerpts. In addition, the index $r_{\mathrm{DAP}}^{\mathrm{PTTV}}$ shows an increase of 9% in AUC compared to $r_{\mathrm{DAP}}^{\mathrm{HRV}}$, which means that detection based on $r_{\mathrm{DAP}}^{\mathrm{PTTV}}$ is more robust and less dependent on detector parameters. As for subjects classification results are the same for $r_{\mathrm{DAP}}^{\mathrm{HRV}}$ and $r_{\mathrm{DAP}}^{\mathrm{PTTV}}$.

PPG and ECG are noninvasive and easily acquired signals. Furthermore, DAP events, HRV, and/or PTTV, which are closely related with apnea can easily be obtained from these electrophysiological signals. The combination of DAP, HRV, and/or PTTV could, therefore, be an alternative for sleep apnea screening with the added benefit of low cost and simplicity. Nevertheless, extended studies are needed to corroborate the potential usefulness of PTTV for evaluating ANS, its relationship with HRV, and its utility in sleep disorder diagnosis.

REFERENCES

[1] C. Guilleminault, A. Tilkian, and W. C. Dement, "The sleep apnea syndromes," *Annu. Rev. Med.*, vol. 27, pp. 465–484, 1976.
[2] R. J. Kimoff, "Sleep fragmentation in obstructive sleep apnea," *Sleep*, vol. 19, no. 9, pp. 219–223, 1996.
[3] F. J. Nieto, T. B. Young, B. K. Lind, E. Shahar, J. M. Samet, S. Redline, R. B. D'Agostino, A. B. Newman, M. D. Lebowitz, and T. G. Pickering, "Association of sleep-disordered breathing, sleep apnea, and hypertension in a large community-based study," *JAMA*, vol. 283, pp. 1829–1836, 2000.
[4] T. Young, P. E. Peppard, and D. J. Gottlieb, "Epidemiology of obstructive sleep apnea," *Amer. J. Respir. Crit. Care Med.*, vol. 165, pp. 1217–1239, 2002.

[5] D. W. Beebe and D. Gozal, "Obstructive sleep apnea and prefrontal cortex: Towards a comprehensive model linking nocturnal upper airway obstruction to daytime cognitive and behavioral deficits," *J. Sleep Res.*, vol. 11, pp. 1–16, 2002.
[6] D. J. Gottlieb, R. M. Vezina, C. Chase, S. M. Lesko, T. C. Heeren, D. E. Weese-Mayer, S. H. Auerbach, and M. J. Corwin, "Symptoms of sleep-disordered breathing in 5-year-old children are associated with sleepiness and problem behaviors," *Pediatrics*, vol. 112, pp. 870–877, 2003.
[7] R. D. Chervin, K. H. Archbold, J. E. Dillon, P. Panahi, K. J. Pituch, R. E. Dahl, and C. Guilleminault, "Inattention, hyperactivity, and symptoms of sleep-disordered breathing," *Pediatrics*, vol. 109, pp. 449–456, 2002.
[8] American Thoracic Society, "Cardiorespiratory sleep studies in children," *Amer. J. Respir. Crit. Care Med.*, vol. 160, pp. 1381–1387, 1999.
[9] Standards of Practice Committee and American Sleep Disorders Association, "Portable recording in the assessment of obstructive sleep apnea," *Sleep*, vol. 17, no. 4, pp. 378–392, 1994.
[10] A. B. Hertzman, "The blood supply of various skin areas as estimated by the photo-electric plethysmograph," *Amer. J. Physiol*, vol. 124, pp. 328–340, 1938.
[11] H. Schneider, C. D. Schaub, C. A. Chen, K. A. Andreoni, A. R. Schwartz, P. L. Smith, J. L. Robotham, and C. P. O'donnell, "Neural and local effects of hypoxia on cardiovascular responses to obstructive apnea," *J. Appl. Physiol.*, vol. 88, pp. 1093–1102, 2000.
[12] U. A. Leuenberger, J. C. Hardy, M. D. Herr, K. S. Gray, and L. I. Sinoway, "Hypoxia augments apnea-induced peripheral vasoconstriction in humans," *J. Appl. Physiol.*, vol. 90, pp. 1516–1522, 2001.
[13] A. Anand, S. Remsburg-Sailor, S. H. Launois, and J. W. Weiss, "Peripheral vascular resistance increases after termination of obstructive apneas," *J. Appl. Physiol.*, vol. 91, pp. 2359–2365, 2001.
[14] V. K. Somers, M. E. Dyken, M. P. Clary, and F. M. Abboud, "Sympathetic neural mechanisms in obstructive sleep apnea," *J. Clin. Invest.*, vol. 96, pp. 1897–1904, 1995.
[15] V. A. Imadojemu, K. Gleeson, K. S. Gray, L. I. Sinoway, and U. A. Leuenberger, "Obstructive apnea during sleep is associated with peripheral vasoconstriction," *Amer. J. Respir. Crit. Care Med.*, vol. 165, pp. 61–66, 2002.
[16] Y. Mendelson, "Pulse Oximetry: Theory and applications for noninvasive monitoring," *Clin. Chem.*, vol. 38, no. 9, pp. 1601–1607, 1992.
[17] M. Nitzan, A. Babchenko, B. Khanokh, and D. Landau, "The variability of the photoplethysmographic signal: A potential method for the evaluation of the autonomic nervous system," *Physiol. Meas.*, vol. 19, pp. 93–102, 1998.
[18] R. P. Schnall, A. Shlitner, J. Sheffy, R. Kedar, and P. Lavie, "Periodic, profound peripheral vasoconstriction-a new marker of obstructive sleep apnea," *Sleep*, vol. 22, no. 7, pp. 939–946, 1999.
[19] A. Bar, G. Pillar, I. Dvir, J. Sheffy, R. P. Schnall, and P. Lavie, "Evaluation of a portable device based on peripheral arterial tone for unattended home sleep studies," *Chest*, vol. 123, pp. 695–703, 2003.
[20] C. P. O'Donnell, L. Allan, P. Atkinson, and A. R. Schwartz, "The effect of upper airway obstruction and arousal on peripheral arterial tonometry in obstructive sleep apnea," *Amer. J. Respir. Crit. Care Med.*, vol. 166, pp. 965–971, 2002.
[21] E. Gil, J. M. Vergara, and P. Laguna, "Detection of decreases in the amplitude fluctuation of pulse photoplethysmography signal as indication of obstructive sleep apnea syndrome in children," *Biomed. Signal Process. Control*, vol. 3, pp. 267–277, 2008.
[22] E. Gil, M. O. Mendez, J. M. Vergara, S. Cerutti, A. M. Bianchi, and P. Laguna, "Discrimination of sleep apnea related decreases in the amplitude fluctuations of PPG signal in children by HRV analysis," *IEEE Trans. Biomed. Eng.*, vol. 56, no. 4, pp. 1005–1014, 2009.
[23] Task Force of The European Society of Cardiology and The North American Society of Pacing Electrophysiology, "Heart rate variability: Standards of measurement, physiological interpretation, and clinical use," *Eur. Heart J.*, vol. 17, pp. 354–381, 1996.
[24] J. E. Naschitz, R. Bezobchuk, R. Mussafia, S. Sundick, D. Dreyfuss, I. Khorshidi, A. Karidis, H. Manor, M. Nagar, E. R. Peck, S. Peck, S. Storch, I. Rosner, and L. Gaitini, "Pulse transit time by r-wave-gate infrared photoplethysmography: Review of the literature and personal experience," *J. Clin. Monit. Comput.*, vol. 18, pp. 333–342, 2004.
[25] J. Y. A. Foo and C. S. Lim, "Pulse transit time as an indirect marker for variations in cardiovascular related reactivity," *Technol. Health Care*, vol. 14, pp. 97–108, 2006.
[26] D. J. Pitson, A. Sandell, R. van den Hout, and J. R. Stradling, "Use of the pulse time as a measure of inspiratoy effort in patients with obstructive sleep apnea," *Eur. Respir. J.*, vol. 8, pp. 1669–1674, 1995.

[27] J. Argod, J. L. Pépin, R. P. Smith, and P. Lévy, "Comparison of esophageal pressure with pulse transit time as a measure of respiratory effort for scoring obstructive nonapneic respiratory events," *Amer. J. Respir. Crit. Care Med.*, vol. 162, pp. 87–93, 2000.

[28] J. Pagani, M. P. Villa, G. Calcagnini, A. Alterio, R. Ambrosio, F. Censi, and R. Ronchetti, "Pulse transit time as a measure of inspiratory effort in children," *Chest*, vol. 124, pp. 1487–1493, 2003.

[29] D. Pitson, N. Chhina, S. Knijn, M. van Herwaaden, and J. Stradling, "Changes in pulse transit time and pulse rate as markers of arousal from sleep in normal subjects," *Clin. Sci. (Lond.)*, vol. 87, pp. 269–273, 1994.

[30] D. Poyares, C. Guilleminault, A. Rosa, M. Ohayon, and U. Koester, "Arousal, EEG spectral power and pulse transit time in UARS and mild OSAS Subjects," *Clin. Neurophysiol.*, vol. 113, pp. 1598–1606, 2002.

[31] E. S. Katz, J. Lutz, C. Black, and C. L. Marcus, "Pulse transit time as a measure of arousal and respiratory effort in children with sleep-disordered breathing," *Pediatr. Res.*, vol. 53, no. 4, pp. 580–588, 2003.

[32] J. Argod, J. L. Pépin, and P. Lévy, "Differentiating obstructive and central sleep respiratory events through pulse transit time," *Amer. J. Respir. Crit Care Med.*, vol. 158, pp. 1778–1783, 1998.

[33] D. J. Pitson and J. R. Stradling, "Value of beat-to-beat blood pressure changes, detected by pulse transit time, in the management of the obstructive sleep apnoea/hypopnoea syndrome," *Eur. Respir. J.*, vol. 12, pp. 685–692, 1998.

[34] J. L. Pépin, N. Delavie, I. Pin, C. Deschaux, J. Argod, M. Bost, and P. Lévy, "Pulse transit time improves detection of sleep respiratory events and microarousals in children," *Chest*, vol. 127, pp. 722–730, 2005, DOI:10.1378/chest.127.3.722.

[35] J. Y. A. Foo, S. J. Wilson, A. P. Bradleyand, G. R. Williams, M. A. Harris, and D. M. Cooper, "Use of pulse transit time to distinguish respiratory events from tidal breathing in sleeping children," *Chest*, vol. 128, pp. 3013–3019, 2005.

[36] A. C. Guyton and J. E. Hall, *Textbook of Medical Physiology*.   New York: Elsevier, 2006, ch. 18, ser. ISBN 0-7216-0240-1.

[37] E. Kandel, J. Schwartz, and T. Jessell, *Principles of Neural Science.*   New York: McGraw-Hill, 2000, ch. 49, ser. ISBN 0-8385-7701-6.

[38] American Thoracic Society, "Standards and indications for cardiopulmonary sleep studies in children," *Amer. J. Respir. Crit. Care Med.*, vol. 153, pp. 866–878, 1996.

[39] J. P. Martinez, R. Almeida, S. Olmos, A. P. Rocha, and P. Laguna, "A wavelet-based ECG delineator: Evaluation on standard databases," *IEEE Trans. Biomed. Eng.*, vol. 51, no. 4, pp. 570–581, Apr. 2004.

[40] M. O. Mendez, A. M. Bianchi, N. Montano, V. Patruno, E. Gil, C. Mantaras, S. Aiolfi, and S. Cerutti, "On arousal from sleep: Time-frequency analysis," *Med. Biol. Eng. Comput.*, vol. 46, pp. 341–351, 2008. DOI:10.1007/s11517-008-0309-z.

[41] C. L. Marcus, "Sleep-disordered breathing in children," *Amer. J. Respir. Crit. Care Med.*, vol. 164, pp. 16–30, 2001.

[42] T. Ma and Y. T. Zhang, "Spectral analysis of pulse transit time variability and its coherence with other cardiovascular variabilities," in *Proc. 28th Annu. Int. Conf. IEEE EMBS*, 2006, pp. 6442–6445.

[43] J. Allen, "Photoplethysmography and its application in clinical physiological measurement," *Physiol. Meas.*, vol. 28, pp. R1–R39, 2007. DOI:10.1088/0967-3334/28/3/R01.

[44] R. G. Norman, I. Pal, C. Stewart, J. A. Walsleben, and M. D. Rapoport, "Interobserver agreement among sleep scorers from different centers in a large dataset," *Sleep*, vol. 23, pp. 901–908, 2000.

[45] P. O. Bridevauxa, J. W. Fittinga, J. M. Fellratha, and J. D. Auberta, "Interobserver agreement on apnoea hypopnoea index using portable monitoring of respiratory parameters," *Swiss Med. Weekly*, vol. 137, pp. 602–607, 2008.

[46] M. S. Schechter, "Technical report: Diagnosis and management of childhood obstructive sleep apnea syndrome," *Pediatrics*, vol. 109, pp. e69–e69, 2002.

[47] R. T. Brouillette, A. Morielli, A. Leimanis, K. A. Waters, R. Luciano, and F. M. Ducharme, "Nocturnal pulse oximetry as an abbreviated testing modality for pediatric obstructive sleep apnea," *Pediatrics*, vol. 105, pp. 405–412, 2000.

[48] T. Penzel, J. McNames, P. de Chazal, B. Raymond, A. Murray, and G. Moody, "Systematic comparison of different algorithms for apnoea detection based on electrocardiogram recordings," *Med. Biol. Eng. Comput.*, vol. 40, pp. 402–407, 2002.

[49] R. B. Shouldice, L. M. O'Brien, C. O'Brien, P. Chazal, D. Gozal, and C. Heneghan, "Detection of obstructive sleep apnea in pediatric subjects using surface lead electrocardiogram features," *Sleep*, vol. 27, no. 4, pp. 784–791, 2004.

[50] G. M. Nixon and R. T. Brouillette, "Diagnostic techniques for obstructive sleep apnoea: Is polysomnography necessary?" *Paediatr. Respir. Rev.*, vol. 3, pp. 18–24, 2002.

[51] American Academy of Pediatrics, "Clinical practice guideline: Diagnosis and management of childhood obstructive sleep apnea syndrome," *Pediatrics*, vol. 109, pp. 704–712, 2002.

Eduardo Gil was born in Zaragoza, Spain, in 1978. He received the M.S. degree in telecommunication engineering and the Ph.D. degree in biomedical engineering from the University of Zaragoza (UZ), Zaragoza, Spain, in 2002 and 2009, respectively, and the Master's degree "Master universitario en Sueño: Fisiología y Medicina" from the University Pablo Olavide of Sevilla, Spain, in 2007.

Since 2006, he has been an Assistant Professor with the UZ, where he is currently a Researcher with the Aragón Institute for Engineering Research and also with the Biomedical Research Networking Center in Bioengineering, Biomaterials and Nanomedicine. His current research interests include the field of biomedical signal processing, specially in the analysis of the photopletismography signal for obstructive sleep apnea diagnosis.

Raquel Bailón was born in Zaragoza, Spain, in 1978. She received the M.Sc. degree in telecommunication engineering and the Ph.D. degree in biomedical engineering from the University of Zaragoza (UZ), Zaragoza, Spain, in 2001 and 2006, respectively.

Since 2003, she has been an Assistant Professor with the Department of Electronic Engineering and Communications, UZ, where she is a Researcher with the Aragón Institute for Engineering Research and also with the Biomedical Research Networking Center in Bioengineering, Biomaterials and Nanomedicine. Her current research interests include the biomedical signal processing field, specially in the analysis of the dynamics and interactions of cardiovascular signals.

José María Vergara was born in Vitoria, Spain, in 1952. He received the M.D. and Ph.D. degrees from the University of Zaragoza, Zaragoza, Spain, in 1977 and 1990, respectively.

Since 1981, he has been a Clinical Neurophysiologist with the Miguel Servet Children's Hospital, Zaragoza. He is currently an Associate Professor with the University of Zaragoza. His research interests include the field of sleep and q-EEG.

Pablo Laguna (M'92–SM'06) was born in Jaca, Huesca, Spain, in 1962. He received the M.S. degree in physics and Ph.D. degree in physic science from the Science Faculty, University of Zaragoza, Zaragoza, Spain, in 1985 and 1990, respectively.

He is a Full Professor of signal processing and communications with the Department of Electrical Engineering, Engineering School, University of Zaragoza, where he is a Researcher with the Aragón Institute for Engineering Research. He is also a member of the Spanish Center for Biomedical Engineering, Biomaterial and Nanomedicine Research. From 1992 to 2005, he was an Associate professor with the University of Zaragoza. From 1987 to 1992, he was an Assistant Professor of automatic control with the Department of Control Engineering, Politecnic University of Catalonia (U.P.C.), Spain, and also a Researcher with the Biomedical Engineering Division of the Institute of Cybernetics (U.P.C.-C.S.I.C.). He has authored or coauthored more than 60 research papers on this topic. Together with L. Sörnmo, he is the author of *Bioelectrical Signal Processing in Cardiac and Neurological Applications* (Elsevier, 2005). His current research interests include signal processing, in particular applied to biomedical applications.